

Be Foil "Filter Knee Imaging" NSTX Plasma with Fast Soft X-Ray Camera

B.C. Stratton¹, S. von Goeler¹, D. Stutman², K. Tritz², and L.E. Zakharov¹

¹*Princeton Plasma Physics Laboratory, Princeton, New Jersey, USA*

²*Johns Hopkins University, Baltimore, Maryland, USA*

A fast soft x-ray (SXR) pinhole camera has been implemented on the National Spherical Torus Experiment (NSTX) [1, 2]. This paper presents observations and describes the Be foil Filter Knee Imaging (FKI) technique for reconstructions of a $m/n=1/1$ mode on NSTX.

The SXR camera has a wide-angle (28°) field of view of the plasma as shown in Figs. 1a and 1b. The camera images nearly the entire diameter of the plasma and a comparable region in the vertical direction. SXR photons pass through a beryllium foil and are imaged by a pinhole onto a P47 scintillator deposited on a fiber optic faceplate. An electrostatic image intensifier demagnifies the visible image by 6:1 to match it to the size of the charge-coupled device (CCD) chip. A pair of lenses couples the image to the CCD chip.

The ultra-fast CCD camera (model PSI-5 produced by Princeton Scientific Instruments, Inc.) is capable of frame rates up to 500 kHz for 300 frames. The camera produces 64 X 64 pixel images. Good images of NSTX plasmas have been obtained at frame rates up to 500 kHz, depending on the intensity of the SXR emission.

The pinhole diameter and Be foil thickness can be varied to change the signal level and low energy cutoff of the imaged SXR photons. A 3 mm diameter pinhole and $7.6 \mu\text{m}$ Be foil were used for the measurements presented here. Fig. 2 shows the transmission curve $F_{Be}(h\nu)$ of this foil, which has a "filter knee" in the 0.5-1.5 keV region.

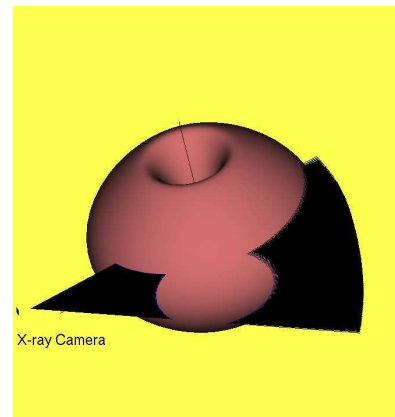


Fig. 1a Field of view of SXR camera.

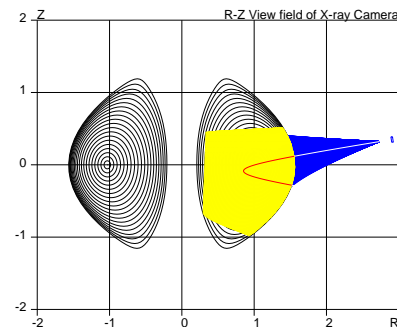


Fig. 1b Field of view in R-Z plane.

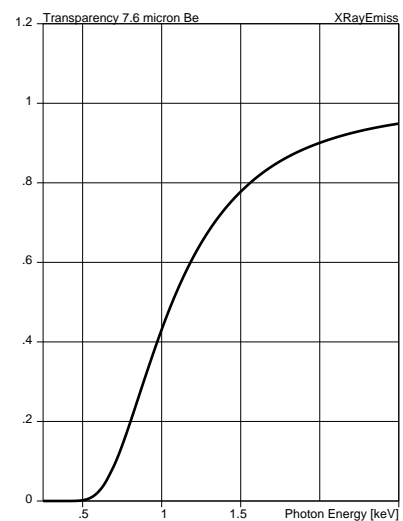


Fig. 2 $F_{Be}(h\nu)$ curve of the Be foil.

The signal S detected by a pixel of the camera is reproduced by the line integral

$$S = \int_t^{t+\delta t} dt \int dh\nu \int_L F_{Be}(h\nu) \mathcal{E}_{h\nu}(T_e, Z_{eff}, n_e, \dots) \frac{dV}{dL} dL \equiv \int_L \mathcal{E}(\dots) \frac{dV}{dL} dL, \quad (1)$$

where the time integration dt is performed over δt , the camera integration time, the second integration is over the photon energy $h\nu$, and the chord integration dL is weighted with the derivative $\frac{dV}{dL}$ of the volume of the sight-line cone with respect to the distance L from the pin hole. The emissivity $\mathcal{E}_{h\nu}(T_e, Z_{eff}, n_e, \dots)$ depends on numerous local parameters in the plasma, including electron temperature T_e and density n_e , effective charge Z_{eff} , recombination, and line emission of impurities. The source function $\mathcal{E}(\dots)$, introduced here, absorbs all integrals except the sight line integration.

The reconstruction of plasma parameters from integral Eq.(1) represents a complicated problem, which involves (a) inversion of the integral equation for $\mathcal{E}(\dots)$ as a function of space coordinates, and (b) inversion of the $\mathcal{E}(\dots)$ function. While the first problem can be solved in the future with, e.g., two spatially separated x-ray cameras, the second step in the reconstruction is problematic for plasmas containing impurities because of a number of unknowns affecting the plasma emissivity.

At the same time, SXR camera data in certain NSTX plasma regimes has clearly shown signals corresponding to fast, time dependent events happening near the plasma center. It was realized during image reconstruction in these cases that significant simplification of the problem is possible when the plasma temperature is below the Be filter knee. In these cases, the foil significantly amplifies the contrast of the plasma center and visibility of perturbative structures associated with the MHD modes. We refer to this as ‘‘Filter Knee Imaging’’, or FKI. Although for the particular choice of the foil thickness used here these (Ohmic) discharges have low temperature, they illustrate the possibility of reconstructing certain structures inside the plasma using FKI.

For the purpose of FKI reconstruction, a special code (Cbbst) was written to simulate the line integral (1) and to make its inversion assuming a simple dependence of $\mathcal{E} = \mathcal{E}(a + \xi)$, where a is a label of the magnetic surfaces corresponding to the normalized square root of the toroidal magnetic flux. The perturbation $\xi(a, \theta, \varphi)$ of magnetic surfaces may include both ideal and tearing types of perturbations. At present, only step-like $m/n=1/1$ perturbations were considered for reconstruction purposes. The 21 radial values of the $\mathcal{E}(a_i)$ function, the amplitude and the phase of the $\xi_{1/1}$ perturbation are reconstructed from the 64×64 data array S_{ij} using the singular value decomposition technique together with an iterative technique for solving the integral equation (1), which becomes non-linear in the presence of perturbations.

The SXR camera data were obtained in an ohmically-heated helium discharge (Shot #113355) at $B_{tor} = 0.44$ T and $I_{pl} = 500$ kA, with $T_e(0) = 0.5$ keV and $n_e(0) = 0.4 \cdot 10^{20} \text{ m}^{-3}$. This shot exhibits a low frequency ($\simeq 2$ kHz) internal mode visible on a conventional central chord SXR diode (5 mm Be foil) as shown in Fig. 3. The mode grows to maximum amplitude in $\simeq 2$ ms and decays in $\simeq 30$ ms.

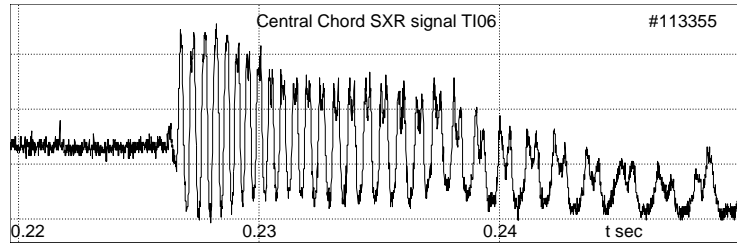


Fig. 3. Waveform of the signal from the SXR detector.

The NSTX magnetic configuration was generated by the Equilibrium and Stability Code [3] using a plasma boundary reconstructed by the EFIT code and TRANSP code simulations of plasma pressure and q profiles, as shown in Fig. 4a. Fig. 4b shows an example of a reconstructed “emissivity” function $\mathcal{E}(a)$ together with its shift due to a $m/n=1/1$ internal perturbation.

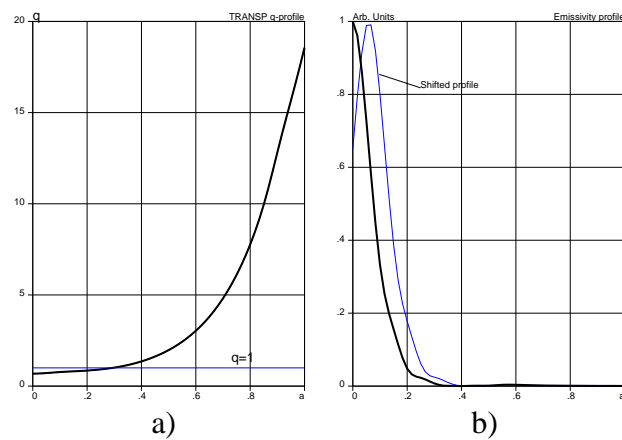


Fig. 4. a) q -profile. b) $\mathcal{E}(a)$ function.

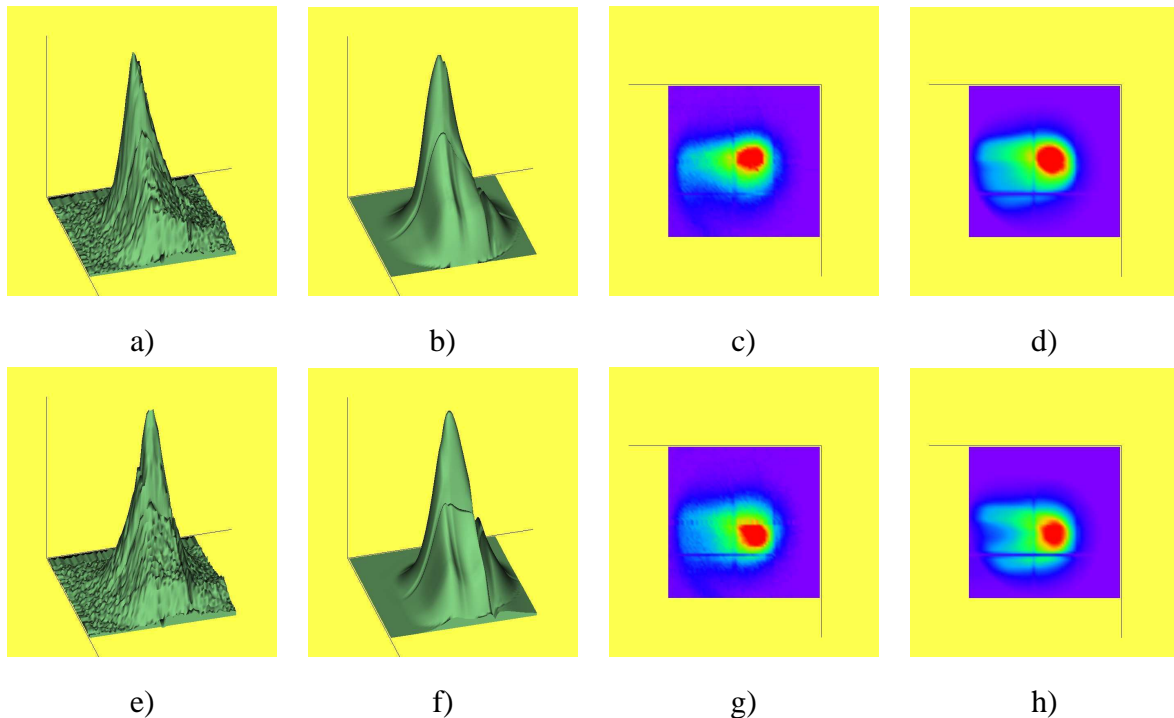


Fig. 5. SXR camera image (64x64 pixel) and its reconstruction by the Cbbst code.

Fig. 5a shows the 3-D plot of the amplitude of the measured image signal on the 64x64 pixel camera screen (with background level subtracted), and Fig. 5b shows its Cbbst reconstruction. Figs. 5c and 5d represent colored top views of the same plots.

Figs 5e - 5h show the corresponding signal and its reconstruction 0.3 ms later demonstrating the change in phase of the $m/n=1/1$ perturbation, when Figs 5g, 5h are compared with Figs 5c, 5d.

In conclusion, we have demonstrated that the FKI technique allows reliable reconstruction of core MHD perturbations in NSTX plasmas. In the future we will use thicker Be foils as well to apply this technique to hotter ($T_e > 1$ keV) NSTX plasmas and to more complicated MHD perturbations.

This work was supported by the U.S. DOE, Contract No. DE-AC02-76CH03073.

References

- [1] S. von Goeler et al., Rev. Sci. Instrum. **70** (1999) 599.
- [2] B. C. Stratton et al., Rev. Sci. Instrum. **75** (2004) 3959.
- [3] L. E. Zakharov and A. Pletzer, Phys. Plasmas **6** (1999) 4693.